

A decentralized control technique for vehicle chassis control

Carlos Villegas, Yin-Lam Chow, Martin Corless, Robert Shorten and Wynita Griggs

Abstract—We present a decentralised control design that is based upon the Kalman-Yakubovich-Popov lemma. We use our technique to design an integrated chassis controller.

I. INTRODUCTION

Decentralized control is an essential feature of control engineering practice. Most real complex systems are controlled using a number of control systems, each designed to control a particular sub-process. Our objective in this paper is to develop one such method that is based on frequency domain design techniques. In particular, we present a passivity based design method that is suitable for the design of decentralized controllers for applications where robustness to sensor failure is a concern [1]. Our approach is based on a novel use of the Kalman-Yakubovich-Popov lemma, and the use of DK-iterations to provide a method for controller design. An advantage of this approach over competing LMI based design methodologies is that uncertainty can be captured in terms of frequency domain models, and that output feedback controllers can easily be designed. We then apply the techniques developed to an automotive application; namely, to track the lateral and vertical motions of the vehicle in order to emulate a reference vehicle.

II. BASIC IDEA

Our starting point is to consider a plant composed of two interacting subsystems. The main objective is to find a decentralized control structure that simultaneously stabilises not only each subsystem but also the full interacting plant with respect to both parameter uncertainty and structural perturbations. A basic mechanism for achieving this objective is to select the feedback structures such that the linearized closed loop system admits a block-diagonal Lyapunov function. Roughly speaking, this problem can be described as follows. Let $A \in \mathbb{R}^{n \times n}$ be a Hurwitz stable (closed loop system) matrix with

$$A = \begin{bmatrix} A_{11} & A_{12} \\ A_{21} & A_{22} \end{bmatrix}, \quad (1)$$

and where both $A_{11} \in \mathbb{R}^{m \times m}$ and $A_{22} \in \mathbb{R}^{(n-m) \times (n-m)}$ are assumed to be Hurwitz stable. The question is whether

This work was supported by SFI grant 07/IN.1/I901, SFI Investigator Award 04/IN.1/I478 and EU Strep CeMACS.

C. Villegas was with the Hamilton Institute and is now with Wavebob Ltd., Maynooth, Ireland carlos@villegasramos.net

M. Corless and Y.-L. Chow are with the School of Aeronautics and Astronautics, Purdue University, West Lafayette, IN 47907, USA

R. Shorten and W. Griggs are with the Hamilton Institute, NUI Maynooth, Ireland

one can find a symmetric, positive-definite, block diagonal matrix

$$P = \begin{bmatrix} P_{11} & 0 \\ 0 & P_{22} \end{bmatrix} \quad (2)$$

such that $A^T P + P A < 0$. The block diagonal nature of P implies that $A_{11}^T P_{11} + P_{11} A_{11} < 0$ and $A_{22}^T P_{22} + P_{22} A_{22} < 0$. In this section, we present two equivalent conditions for block diagonal stability: a passivity condition and a small-gain condition. The passivity condition was first suggested in [2] in the context of diagonal stability, and in [3] in the context of automotive dynamics. The small gain condition profits from the well-known connection between passivity and the small-gain theorem [4]. We begin with the following theorem on block diagonal stability [1].

Theorem 2.1: The following statements are equivalent for a square 2×2 block matrix A with the structure given in (1).

- (i) The system $\dot{x} = Ax$ is block-diagonally stable.
- (ii) The matrix A_{11} is Hurwitz and there exists a matrix $P_{22} = P_{22}^T > 0$ such that the transfer function $-P_{22}G$ is ESPR (extended strictly positive real [1]) where

$$G(s) = A_{22} + A_{21}(sI - A_{11})^{-1}A_{12}.$$

- (iii) The matrix $A_{h11} = A_{11} + A_{12}(I - A_{22})^{-1}A_{21}$ is Hurwitz and there exists a constant nonsingular matrix D such that $\|DHD^{-1}\|_\infty < 1$ where

$$H = (G + I)(G - I)^{-1}.$$

Comment: Consider the system $\dot{x} = Ax$ where $x^T = [x_1^T, x_2^T]$ and A is given by (1). Defining input $w = x_2$ and output $z = \dot{x}_2$ we obtain the following input-output system:

$$\begin{aligned} \dot{x} &= A_{11}x + A_{12}w \\ z &= A_{21}x + A_{22}w \end{aligned} \quad (3)$$

Clearly, the transfer function G in the above passivity characterization of block diagonal stability is the transfer function of this system, that is, G is the transfer function from x_2 to \dot{x}_2 . If we now introduce new input and output variables

$$\begin{aligned} w_h &:= (w - z)/\sqrt{2} = (x_2 - \dot{x}_2)/\sqrt{2} \\ z_h &:= (-w - z)/\sqrt{2} = (-x_2 - \dot{x}_2)/\sqrt{2} \end{aligned} \quad (4)$$

then,

$$\begin{aligned} w &= (w_h - z_h)/\sqrt{2} \\ z &= (-w_h - z_h)/\sqrt{2} \end{aligned} \quad (5)$$

and one can readily show that the transfer function $H = (G + I)(G - I)^{-1}$ in the above small gain characterization of block diagonal stability is the transfer function from w_h to z_h .

A. Example

The above result can be used in some situations to obtain a more computationally efficient method of determining block diagonal stability. Suppose for example that the number m of state variables in the first subsystem is large and the number $m_2 := n - m$ of state variables in the second subsystem is relatively small. One can check block diagonal stability by determining whether or not the associated LMI is feasible with a symmetric block diagonal matrix $P = \text{diag}(P_{11}, P_{22})$ satisfying $P > 0$. Since P_{11} is a symmetric $m \times m$ matrix, it involves a large number $(m(m + 1)/2)$ of independent variables; P_{22} involves $m_2(m_2 + 1)/2$ independent variables. Also, this LMI has a large dimension of $n \times n$. However the equivalent frequency domain condition in (iii) of the above theorem is equivalent to the existence of a symmetric matrix $P_{22} > 0$ such that

$$H(j\omega)^* P_{22} H(j\omega) - P_{22} < 0 \quad (6)$$

for all $\omega \in \mathbb{R} \cup \{\infty\}$. Although this is an infinite number of LMIs, one can choose a finite number of frequencies $\omega_1, \dots, \omega_N$ with $\omega_N = \infty$ and determine the feasibility of

$$H(j\omega_k)^* P_{22} H(j\omega_k) - P_{22} < 0, \quad \text{for } k = 1, \dots, N. \quad (7)$$

In these LMIs, the number of independent variables is low $(m_2(m_2 + 1)/2)$. Thus, it may be computationally more efficient to determine the feasibility of (7) for a reasonable number of frequencies rather than the original LMI. To illustrate, we randomly generated a block diagonally stable system in which $m = 100$ and $m_2 = 2$. Computations were carried out using the software packages YALMIP and MATLAB 2010(a) on a laptop equipped with an Intel Core 2 Duo P8800 CPU. It took about 50 seconds to determine the feasibility of the Lyapunov LMI (which involves 5053 variables) while it only took about 7.6 sec to determine the feasibility of the frequency domain LMIs using 501 frequencies; 500 frequencies were chosen between 0 and 5000 and one point at infinity. Using 11 frequencies, the computation only took about 0.33 seconds. The frequency domain LMIs only involve 3 variables. To demonstrate that the P_{22} matrices found using a finite number of frequencies, do indeed guarantee satisfaction of the frequency domain inequalities for all frequencies, and to illustrate item (ii) of the above theorem, we depict $\lambda(\omega)$ in Figures 1 and 2 where $\lambda(\omega)$ is the minimum eigenvalue of $-P_{22}G(j\omega) - G(j\omega)^* P_{22}$. Note that this quantity should be positive for all ω which indeed it is.

III. CONTROL DESIGN

Consider the plant illustrated in Figure 3(a) which has two control inputs u_1, u_2 and two measured outputs y_1, y_2 .

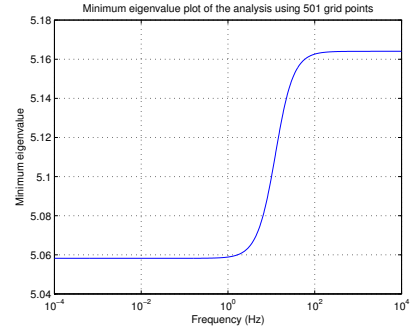


Fig. 1. Plot of λ for P_{22} obtained with 501 frequency grid points

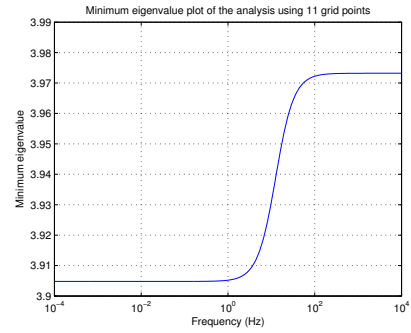


Fig. 2. Plot of λ for P_{22} obtained with 11 frequency grid points

For $i = 1, 2$, each subsystem G_i of the plant is associated with an input u_i and an output y_i . The controller K_1 is required to stabilise subsystem one and controller K_2 is required to stabilise subsystem two. The problem is to find K_1 to stabilise the plant \tilde{G} (with a given K_2 in the loop) such that the overall system is block diagonally stable (see Figure 3(b)).

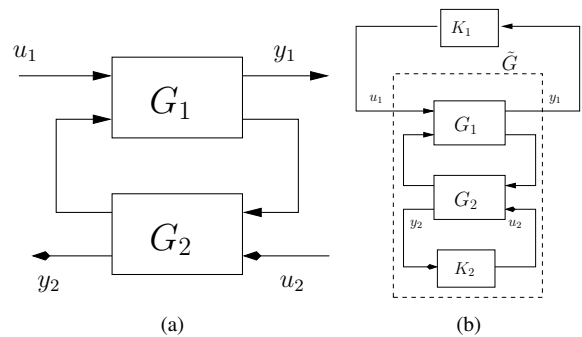


Fig. 3. (a) 2-block decentralized output-feedback control problem. (b) For a given controller K_2 , the problem may be seen as finding a stabilizing controller K_1 for virtual plant \tilde{G} .

Suppose that the plant \tilde{G} with K_2 in the loop has state $[x_1^T \ x_2^T]^T$, control input u_1 , output y_1 and is described by

$$\begin{aligned} \dot{x}_1 &= A_{11}x_1 + A_{12}x_2 + B_{11}u_1 \\ \dot{x}_2 &= A_{12}x_1 + A_{22}x_2 + B_{21}u_1 \\ y_1 &= C_{11}x_1 + C_{12}x_2 + D_{11}u_1 \end{aligned}$$

In what follows we shall identify a system with its system matrix. The system matrix for the plant \tilde{G} is given by

$$\left[\begin{array}{cc|c} A_{11} & A_{12} & B_{11} \\ A_{21} & A_{22} & B_{21} \\ \hline C_{11} & C_{12} & D_{11} \end{array} \right] : \tilde{G}. \quad (8)$$

Introducing the variables $w = x_2$ and $z = \dot{x}_2$, the corresponding system \hat{G} with state x_1 , input (w, u_1) and output (z, y_1) has the following system matrix:

$$\left[\begin{array}{c|cc} A_{11} & A_{12} & B_{11} \\ \hline A_{21} & A_{22} & B_{21} \\ C_{11} & C_{12} & D_{11} \end{array} \right] : \hat{G}. \quad (9)$$

Consider this plant subject to controller $u_1 = K_1 y_1$ and let $\mathcal{F}_\ell(\tilde{G}, K_1)$ be the transfer function from w to z of the resulting closed loop system. It now follows from Theorem 2.1, that the closed-loop system resulting from controller K_1 applied to plant \tilde{G} described in (8) is block diagonally stable if and only if K_1 stabilizes the plant \hat{G} and there exists a positive symmetric matrix P_{22} such that

$$\hat{G}_{SPR} \text{ is ESPR} \quad (10)$$

where

$$\hat{G}_{SPR} := -P_{22}\mathcal{F}_\ell(\hat{G}, K_1) \quad (11)$$

Recall the variables w_h and z_h and let \hat{H} be the system corresponding to the the plant \hat{G} with state x_1 , input (w_h, u_1) and output (z_h, y_1) . Then, one may readily show that \hat{H} has the following system matrix:

$$\left[\begin{array}{c|cc} A_{h11} & A_{h12} & B_{h11} \\ \hline A_{h21} & A_{h22} & B_{h21} \\ C_{h11} & C_{h12} & D_{h11} \end{array} \right] : \hat{H} \quad (12)$$

where

$$\begin{aligned} A_{h11} &= A_{11} + A_{12}(I - A_{22})^{-1}A_{21}, \\ A_{h12} &= \sqrt{2}A_{12}(I - A_{22})^{-1} \\ A_{h21} &= \sqrt{2}(A_{22} - I)^{-1}A_{21}, \\ A_{h22} &= (A_{22} - I)^{-1}(A_{22} + I) \\ B_{h11} &= B_{11} - A_{12}(I - A_{22})^{-1}B_{21}, \\ B_{h21} &= (A_{22} - I)^{-1}B_{21} \\ C_{h11} &= C_{11} - C_{12}(A_{22} - I)^{-1}A_{21}, \\ C_{h12} &= C_{12} - C_{12}(A_{22} - I)^{-1}(A_{22} + I) \\ D_{h11} &= D_{11} - C_{12}(A_{22} - I)^{-1}B_{21} \end{aligned} \quad (13)$$

Consider this plant subject to controller $u_1 = K_1 y_1$ and let $\mathcal{F}_\ell(\hat{H}, K_1)$ be the transfer function from w_h to z_h of the resulting closed loop system. We now obtain the following result from Theorem 2.1.

The closed-loop system resulting from controller K_1 applied to the plant \tilde{G} described in (8) is block diagonally stable if and only if K_1 stabilizes the plant \hat{H} and there exists a nonsingular matrix D such that

$$\|D\mathcal{F}_\ell(\hat{H}, K_1)D^{-1}\|_\infty < 1 \quad (14)$$

Finally, a K_1 and D are found iteratively by solving the condition in (14) with an approach similar to the standard

D-K iteration: for an initial D (such as $D = I$) a K_1 is found to minimize the \mathcal{H}_∞ norm $\|D\mathcal{F}_\ell(\hat{H}, K_1)D^{-1}\|_\infty$ using standard robust control techniques, then a single D is found also to minimize $\|D\mathcal{F}_\ell(\hat{H}, K_1)D^{-1}\|_\infty$. This procedure is repeated until the inequality in (14) is satisfied. A procedure based on this idea is presented in the next section.

IV. ITERATIVE DESIGN METHODOLOGY

A general practical design procedure is now presented. It is analogous to the well known D-K iteration method with constant D-scaling matrices used in μ -synthesis [5]. This procedure to design a controller K_1 for a given K_2 is summarized in the following steps:

- (i) Choose an initial estimate of the scaling matrix D .
- (ii) Solve an H_∞ -optimization problem to minimize $\|D\mathcal{F}_\ell(\hat{H}, K_1)D^{-1}\|_\infty$ over all stabilizing K_1 's. Let its minimizing controller be denoted by \hat{K}_1 .
- (iii) Minimize $\bar{\sigma}(D\mathcal{F}_\ell(\hat{H}, \hat{K}_1)D^{-1})$ for a single nonsingular matrix D across all frequencies. Note that this time, the controller \hat{K}_1 from the last step is being used. The minimization produces a new scaling matrix D denoted as \hat{D} .
- (iv) Compare \hat{D} with the previous estimate D . Stop if they are close. Otherwise, replace D with \hat{D} and return to step (ii).

The closed-loop system is block-diagonal stable if $\|\hat{D}\mathcal{F}_\ell(\hat{H}, \hat{K}_1)\hat{D}^{-1}\|_\infty < 1$.

V. DECENTRALISED DESIGN OF AN INTEGRATED CHASSIS CONTROLLER (ICC)

We now apply the design methodology proposed in the previous section to an application from automotive dynamics [6]. Specifically, we consider the design of an integrated chassis controller for application to vehicle emulation.

A. The variable dynamics vehicle

The basic objective of vehicle emulation is to recreate the chassis motions of a wide range of virtual and production vehicles. Typically, such vehicles are fitted with 4-wheel-steering and active suspension. The test vehicle performing this task is referred to as a vehicle emulator. In this work, the emulation is constrained to lateral and vertical motions. The lateral motion of a vehicle can be described by the lateral velocity and yaw-rate of its chassis while the vertical motions can be described by its heave, pitch and roll motions [7]. Since lateral motion has no significant influence on heave or pitch, in this work the emulation of vertical motions is constrained to chassis roll. Therefore, the integrated chassis control (ICC) for vehicle emulation described in this paper aims at accurately tracking lateral velocity, yaw-rate and roll of a reference vehicle. The reference motions to be tracked by the vehicle represent the motions of virtual or production vehicles. The vehicles to be emulated range from a small urban vehicle to a large bus.

B. Single track model with roll degree of freedom

Full details of the vehicle model can be found in [1]. Here we give only an overview. The wheels at each axle

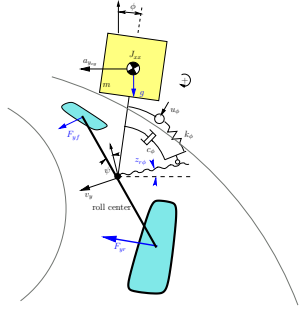


Fig. 4. Single-track model with roll

are lumped together into a single imaginary wheel located at the center of the respective axle. The two resulting imaginary wheels are interconnected by a one-dimensional rigid element acting as a roll axis for the chassis. Pitch, heave and vertical tyre dynamics are neglected. The CoG of the chassis is located at a distance h_{cg} from the roll axis, a distance l_f from the front axle and a distance l_r from the rear axle. It is also assumed that the longitudinal speed v_x is constant and that the only horizontal forces acting on the model are the cornering forces F_{yf} and F_{yr} . Thus, the force acting on the front (rear) wheel of the model corresponds to the combined forces acting on the front (rear) wheels of the vehicle. Finally, the motion of the single-track model with roll degree of freedom is controlled with three control inputs: front and rear steering angles (δ_f, δ_r) and a roll displacement input u_ϕ .

TABLE I
NOTATION

m	Vehicle mass	kg
J_{zz}	Yaw moment of inertia	kg m ²
J_{xx}	Roll moment of inertia	kg m ²
$J_{x_{eq}}$	Roll moment of inertia about roll axis	kg m ²
l_f	Distance from CoG to front wheel center	m
l_r	Distance from CoG to rear wheel center	m
F_{yf}	Front tyre cornering force	N
F_{yr}	Rear tyre cornering force	N
C_f	Front tyre cornering stiffness	N/rad
C_r	Rear tyre cornering stiffness	N/rad
α_f	Front tyre slip angle	rad
α_r	Rear tyre slip angle	rad
c_ϕ	Damping coefficient	N s/m
k_ϕ	Suspension stiffness	N/m
$z_r \phi$	Road bank angle	rad
h_{cg}	Height of CoG	m
g	Acceleration of gravity	m/s ²
v_x	Longitudinal speed	m/s

As mentioned earlier, the lateral motion of the chassis is described by the lateral velocity v_y and yaw-rate $\dot{\psi}$, while the vertical dynamics are described by the roll angle ϕ . Three differential equations govern the motions of the chassis (refer

to Table I for notation):

$$m\dot{v}_y = -mv_x\dot{\psi} + F_{yf} + F_{yr} + mh_{cg}\ddot{\phi} \quad (15)$$

$$J_{zz}\ddot{\psi} = F_{yf}l_f - F_{yr}l_r \quad (16)$$

$$J_{x_{eq}}\ddot{\phi} = (mgh_{cg} - k_\phi)\phi - c_\phi\dot{\phi} + k_\phi u_\phi + mh_{cg}a_y \quad (17)$$

with $a_y = \dot{v}_y + v_x\dot{\psi}$ being measured at the roll center and $J_{x_{eq}} = J_{xx} + mh_{cg}^2$. For small tyre slip angles (α_f, α_r) and neglecting load sensitivity¹, F_{yf} and F_{yr} can be approximated by:

$$F_{yf} = C_f\alpha_f = C_f \left(\delta_f - \frac{v_y + l_f\dot{\psi}}{v_x} \right) \quad (18)$$

$$F_{yr} = C_r\alpha_r = C_r \left(\delta_r - \frac{v_y - l_r\dot{\psi}}{v_x} \right) \quad (19)$$

The model is valid on high friction roads below 0.4g (approximately 4 m/s²) about a constant vehicle speed [7].

Lateral dynamics: When designing controllers for the lateral dynamics of the chassis, it is a common practice to consider only the lateral motion of the vehicle as described by the single-track model. The single-track model is depicted in Figure 5 and its motion is described by the two differential equations:

$$m\dot{v}_y = -mv_x\dot{\psi} + F_{yf} + F_{yr} \quad (20)$$

$$J_{zz}\ddot{\psi} = F_{yf}l_f - F_{yr}l_r \quad (21)$$

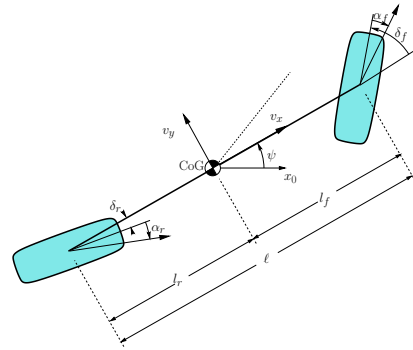


Fig. 5. Single-track model

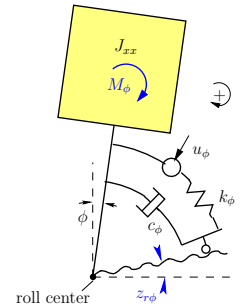


Fig. 6. Roll model

Vertical dynamics: The vertical dynamics are simplified to consider only roll dynamics. We assume that the suspension can be modeled as a passive suspension with a displacement input. The resulting roll model evolves according to the differential equation:

$$J_{xx}\ddot{\phi} = (mgh_{cg} - k_\phi)\phi - c_\phi\dot{\phi} + k_\phi u_\phi + mh_{cg}a_{y_{cg}} \quad (22)$$

where ϕ is the roll angle of the chassis and $a_{y_{cg}}$ is the lateral acceleration at the CoG which is given by $a_{y_{cg}} = \dot{v}_y + v_x\dot{\psi} -$

¹The vertical force at each tyre affect the tyre stiffness. This is referred to as load sensitivity and its effect should be considered for accelerations above 0.4g [8].

$h_{cg}\ddot{\phi}$. The road bank angle $z_{r\phi}$ is neglected for simplicity. Note that there is a strong perturbation coming from the lateral dynamics via the lateral acceleration $a_{y_{cg}}$. In practice, $a_{y_{cg}}$ can be measured so that feed-forward control can be used to cancel the effect of lateral dynamics on roll motion.

C. ICC Design - Simulation results

Our objective now is to design a decentralized controller for a vehicle equipped with 4-wheel-steering and active suspension. Our specific task is to stabilise the lateral and roll dynamics of the vehicle where K_1 stabilises the lateral dynamics, and K_2 the vertical dynamics; and to use the resulting controllers to track a set of reference inputs. While both subsystems clearly affect one another, the requirement for a decentralized structure is a stringent one and comes directly from the automotive manufacturers. A controller for each subsystem was sequentially designed: first the vertical subsystem and then the lateral dynamics at different operating speeds; this latter subsystem is speed-dependent.

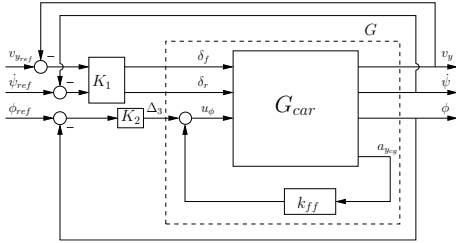


Fig. 7. Vehicle emulation using 2-block decentralized control. The vehicle plant G_{car} is stabilized using an inner feedback loop k_{ff} and a decentralized controller to track the reference lateral velocity v_{yref} , yaw-rate $\dot{\psi}_{ref}$ and roll angle ϕ_{ref} .

The single-track model with roll is a simple model that qualitatively captures the motions of the vehicle chassis dynamics. The model is depicted in Figure 4 and evolves according to (15)-(17) described in Section 2.2.

Consider the controller structure in Figure 7. With such a structure, the plant G_{car} is stabilised by using an inner-loop feedback k_{ff} and a block-diagonal controller

$$K(s) = \begin{bmatrix} K_1(s) & 0 \\ 0 & K_2(s) \end{bmatrix}.$$

The choice of the scalar k_{ff} results in the transformed dynamics G having roll dynamics decoupled from the lateral dynamics. Notice that in the case of failure of the inner-loop k_{ff} , the roll dynamics are not independent of lateral dynamics any more. In such a situation, a controller design based on the decoupling assumption could result in the closed-loop system being unstable. On the other hand, if the controller is designed to provide block-diagonal stability based on the plant with inner-loop failure, such a controller also guarantees the stability of the decoupled case as well.

In order to design a block-diagonal controller consider a roll dynamics PID controller $K_2(s)$ given by

$$K_2(s) = k_d s + k_p + \frac{k_i}{s},$$

with $k_d = .0248$, $k_p = 1.0596$ and $k_i = 13.6429$. This controller stabilises the roll dynamics.

The partial closed-loop system (with only the roll controller K_2 loop closed) and with inner-loop k_{ff} failure ($k_{ff} = 0$) evolves according to:

$$\begin{bmatrix} \dot{x}_1 \\ \dot{x}_2 \end{bmatrix} = \begin{bmatrix} A_{11} & A_{12} \\ A_{21} & A_{22} \end{bmatrix} \begin{bmatrix} x_1 \\ x_2 \end{bmatrix} + \begin{bmatrix} B_{11} \\ B_{21} \end{bmatrix} u_1$$

with

$$\begin{bmatrix} A_{11} & A_{12} \\ A_{21} & A_{22} \end{bmatrix} = \begin{bmatrix} -\frac{J_{xeq}(C_f+C_r)}{J_{xx}mv_x} & -v_x + \frac{J_{xeq}(C_r l_r - C_f l_f)}{J_{xx}mv_x} \\ \frac{(C_r l_r - C_f l_f)}{J_{xx}v_x} & -\frac{C_f l_f^2 + C_r l_r^2}{J_{xx}v_x} \\ -\frac{h_{cg}(C_f+C_r)}{J_{xx}v_x} & \frac{h_{cg}(C_r l_r - C_f l_f)}{J_{xx}v_x} \\ 0 & 0 \\ 0 & 0 \end{bmatrix},$$

$$\begin{bmatrix} B_{11} \\ B_{21} \end{bmatrix} = \begin{bmatrix} \frac{I_{eq}C_f}{J_{xx}m} & \frac{I_{eq}C_r}{J_{xx}m} \\ \frac{C_f l_f}{J_{xx}} & -\frac{C_r l_r}{J_{xx}} \\ \frac{C_f h_{cg}}{J_{xx}} & \frac{C_r h_{cg}}{J_{xx}} \\ 0 & 0 \\ 0 & 0 \end{bmatrix},$$

where $x_1 = [v_y \ \dot{\psi}]^T$, $x_2 = [\ddot{\phi} \ \dot{\phi} \ \phi]^T$, $u_1 = [\delta_f \ \delta_r]^T$.

We now wish to find a state-feedback linear controller $u_1 = K_1(s)x_1$ such that the closed-loop system is block-diagonally stable. From Section III, such a controller may be obtained by finding a matrix D and controller K_1 satisfying:

$$\|D\mathcal{F}_\ell(\hat{H}, K_1)D^{-1}\|_\infty < 1, \quad (23)$$

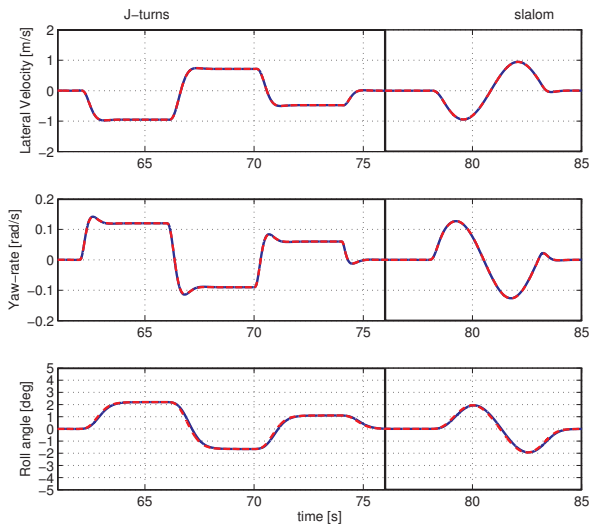
for the system \hat{H} defined in (12).

The D-K iteration described in Section IV was used to find controllers K_1 for three different speeds: 40, 80 and 120 km/h. For example, for 120 km/h, the controller obtained is

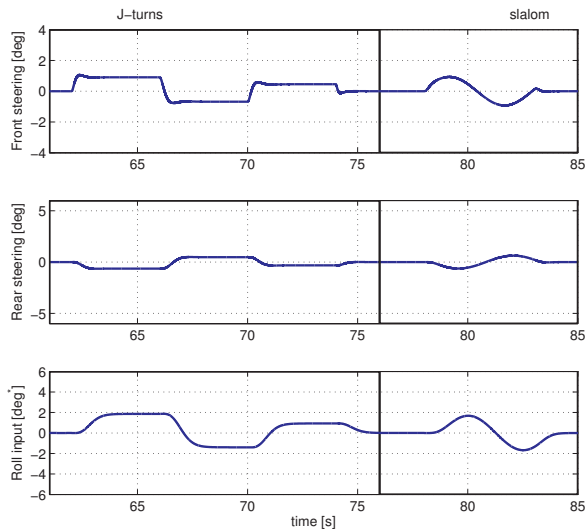
$$K_1(s) = \begin{bmatrix} -\frac{0.11s+0.037}{s} & .1726 \\ \frac{.013s+.02}{s} & -.075 \end{bmatrix}$$

Simulation results for a mid-sized vehicle emulating a light commercial vehicle at 120 km/h are presented in Figure 8. In Figure 8(a), the reference dynamics (dashed) are being tracked by the vehicle outputs (solid) for the selected J-turn and slalom maneuvers. The tracking of reference signals is very good with reference and output signals almost overlapping. The required control inputs are depicted in Figure 8(b). The tracking performance is improved by using a feedforward term. Note that even though performance is not part of the design procedure, good performance is obtained.

In addition, simulation results for a small and more agile Smart for-two vehicle are depicted in Figure 9 for J-turn and slalom maneuvers. Lateral and roll motions are tracked well. Note that in this case, roll reference signals were close to zero because of the very low roll motions of a small urban vehicle.



(a) Lateral velocity, yaw-rate and roll angle tracking



(b) 4-wheel-steering and roll inputs

Fig. 8. Emulation results for a light commercial vehicle at 120km/h using a mid-sized vehicle. (a) Plant outputs (solid) track reference signals (dashed) for a series of maneuvers with a maximum steering wheel rate of 500 deg/s.

VI. CONCLUSION

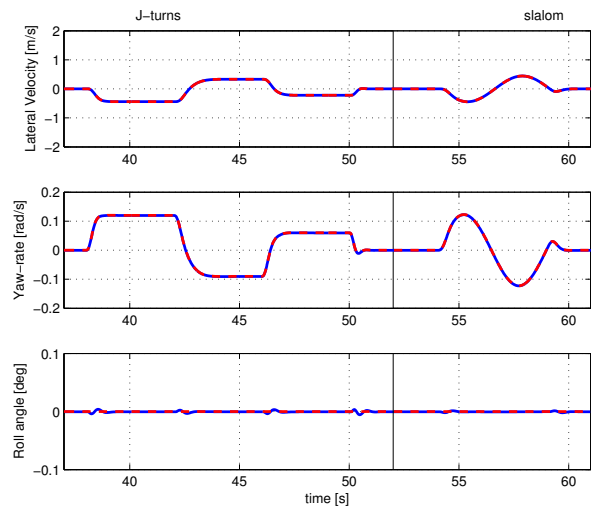
In this paper, based on previous results in [2], a passivity-based design methodology for decentralized control is presented.

VII. ACKNOWLEDGEMENTS

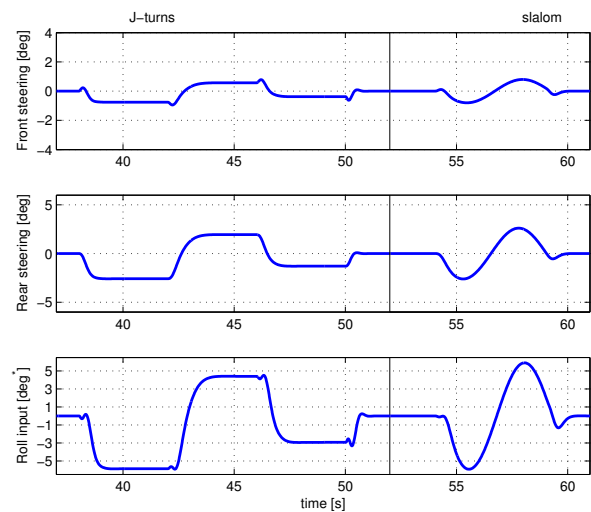
The authors would like to acknowledge the support from Daimler AG within the framework of the CEMACS project.

REFERENCES

- [1] C. Villegas, M. Corless, W. Griggs, and R. Shorten, "A passivity based decentralized control design methodology with application to vehicle dynamics control," *Journal of Dynamic Systems, Measurement and Control*, to appear.
- [2] R. N. Shorten and K. S. Narendra, "Strict positive realness and the existence of diagonal Lyapunov functions," in *2006 45th IEEE Conference on Decision and Control*, San Diego, CA, 2006.



(a) Lateral velocity, yaw-rate and roll angle tracking.



(b) 4-wheel-steering and roll input

Fig. 9. Emulation results for a small urban vehicle using a mid-sized vehicle. (a) Plant outputs (solid) track reference signals (dashed) for a series of maneuvers with a maximum steering wheel rate of 500 deg/s.

- [3] S. Solmaz, "Topics in automotive rollover prevention: Robust and adaptive switching strategies for estimation and control," Ph.D. dissertation, NUI Maynooth, 2007.
- [4] M. Safonov, J. Ly, and R. Chiang, " μ -synthesis robust control: What's wrong and how to fix it?" in *1993 IEEE Conference on Aerospace Control Systems*, Westlake Village, CA, 1993.
- [5] K. Zhou and J. C. Doyle, *Essentials of Robust Control*. Prentice Hall, 1998.
- [6] C. Villegas, M. Readman, M. Akar, and R. Shorten, "Deliverable 21: integrated chassis control," in *CEMACS Project Final Report*, July 2007.
- [7] T. D. Gillespie, *Fundamentals of Vehicle Dynamics*. Society of Automotive Engineers, 1992.
- [8] M. Mitschke and H. Wallentowitz, *Dynamik der Kraftfahrzeuge*. Springer, 2004.